



HAL
open science

Characterization of fracture network based on photogrammetry

Madeline Chapelet, Chrystel Dezayes, Thomas Dewez

► **To cite this version:**

Madeline Chapelet, Chrystel Dezayes, Thomas Dewez. Characterization of fracture network based on photogrammetry. 2019. hal-02390339

HAL Id: hal-02390339

<https://brgm.hal.science/hal-02390339>

Preprint submitted on 3 Dec 2019

HAL is a multi-disciplinary open access archive for the deposit and dissemination of scientific research documents, whether they are published or not. The documents may come from teaching and research institutions in France or abroad, or from public or private research centers.

L'archive ouverte pluridisciplinaire **HAL**, est destinée au dépôt et à la diffusion de documents scientifiques de niveau recherche, publiés ou non, émanant des établissements d'enseignement et de recherche français ou étrangers, des laboratoires publics ou privés.

Characterization of fracture network based on photogrammetry

Madeline Chapelet¹, Chrystel Dezayes¹, Thomas Dewez¹

¹BRGM, French Geological Survey, 3, avenue C. Guillemin, F-45060 Orléans Cedex 2

c.dezayes@brgm.fr

Keywords: Fractures, photogrammetry, geothermal energy, Valence Basin of France

ABSTRACT

Nowadays, deep geothermal exploitation projects in France are mostly localized in deep fractured geological contexts as rift basins. This study contributes to a project aimed at developing a theoretical model of geothermal reservoirs in fault zone in rift areas (grabens) such as the South-East Basin of France. The knowledge of the fracture network and the structural characterization of the potential geothermal reservoirs is essential to the development of a thermo-hydro-mechanical model.

The orientation and spatial organization of the fracture networks in the targeted sedimentary formations have been studied from virtual outcrop models acquired using photogrammetry.

The results have shown that most fractures observed on the outcrop level are oriented in accordance with the 1:50 000 map faults orientation, i.e. NW-SE to NNW-SSE. These local faults are related to the geodynamics events that occurred during the Valence Basin tectonic evolution such as those developed during the Tethysian rifting. The fractures frequency increases with closeness to these main faults. In the first 5 meters from the fault, the fractures are grouped together as a corridor, with a mean spacing S of 25 cm. After that, fractures are regularly located but more spaced ($S > 50$ cm) over several tens meters on both sides of the fault.

All these information can therefore be used as input parameters to the thermo-hydro-mechanical modelling of the geothermal reservoir in order to characterize fluid circulations, heat transfer and to predict the mechanical behavior during the exploitation.

The work conducted in this study also revealed the usefulness and relevance of the use of photogrammetry in analyzing fracture networks at the outcrop level. The virtual outcrop models delivered reliable and complementary measurements to those carried out directly on the field.

1. INTRODUCTION

In France, deep geothermal projects and exploration works are mainly located in basins linked to the West European rift system. One of the rift basins targeted by industrial projects to exploit deep fractured reservoirs is the Valence Basin located in the South-East Basin of France. Within the framework of optimizing the exploitation of deep geothermal energy, we want to refine the implementation of drilling programs by reducing the geological uncertainties. For that, a project is set up with the aims at developing a theoretical model of geothermal reservoirs in fault zone in rift areas. An important feature of developing a thermo-hydro-mechanical model of the reservoir is to understand the fluid circulation by studying the fracture network and its geometry. The better the characterization is, the better the fluid flow modelling expects the fluid pathway and therefore the geological risk is reduced.

Our study have a purpose to make a contribution towards achieving better knowledge about geometry of the fracture network in the reservoir rocks localized in the Valence Basin. The study area lies to the west of the basin, on the eastern border of the Massif Central where Triassic sandstones crops out, which constitutes analogs to the targeted formations. On several accessible quarries, we characterized the fracture network geometry. For that, we use of a ground-based photogrammetric method which consists in taking convergent pictures to cover the walls of the quarries from different locations to compute a 3D virtual geological outcrop based on 3D point cloud. We performed structural data measurements on these virtual outcrop models in order to determine the main fracture sets and their spatial organization.

This work contributes to the main project in providing additional information regarding the potential geothermal reservoirs but it also allows us to evaluate the photogrammetric method relevance for purposes of fracture network characterization at the outcrop scale.

2. GEOLOGICAL CONTEXT

2.1. Geological history of the Valence Basin of France

The Valence Graben is a part of the South-East Basin of France belonging to West European Rifting event (Ziegler, 1992) (Figure 1A). Sediment thickness can reach 6000 m in the center of the Valence Basin (Lienhardt and Pachoud, 1974; Deville *et al.*, 1994), which is mostly filled by Mesozoic and Tertiary sediments (Figure 1B).

During the Hercynian orogeny, the N-S compression resulted in the formation of NE-SW trending sinistral strike-slip faults (Cevennes, Nîmes and Durance Faults) and ENE-WSW to E-W thrust faults (Arthaud and Matte, 1975) (Figure 1A).

A long period of extensional regimes followed, beginning during the Triassic period: the Tethysian rifting. This E-W extension (Bergerat and Martin, 1993) created N30°E and N160°E normal faults (Blès *et al.*, 1989; Martin and Bergerat, 1996). While the Tethys Ocean is forming, the first sediments are deposited in a small neofomed basin. The thermal subsidence replaces the tectonic subsidence at the end of the Jurassic (Lemoine *et al.*, 1986). In the lower Cretaceous, the extensive phase ends and the basin borders undergoes strong erosion (2000 to 2500m thick) (Bonijoly *et al.*, 1996). The subduction of the Tethys Ocean leads to the Pyrenean

collision in the Eocene (Choukroune *et al.*, 1973), which created NNE-SSW sinistral strike-slip faults and NW-SE dextral strike-slip faults (Bergerat, 1982).

The main phase of the Valence Basin opening occurred during the West European Rifting event in Oligocene. This E-W extensive phase fractured all of Western Europe (Ziegler, 1992) and reactivated N-S to NNE-SSW trending tectonic structures. After this large period of sedimentation, the Valence Basin underwent a tectonic inversion during the Alpine compression, which reactivate the normal faults of the Tethysian rifting with reverse movement (Roure *et al.*, 1992, 1994) (Figure 1B).

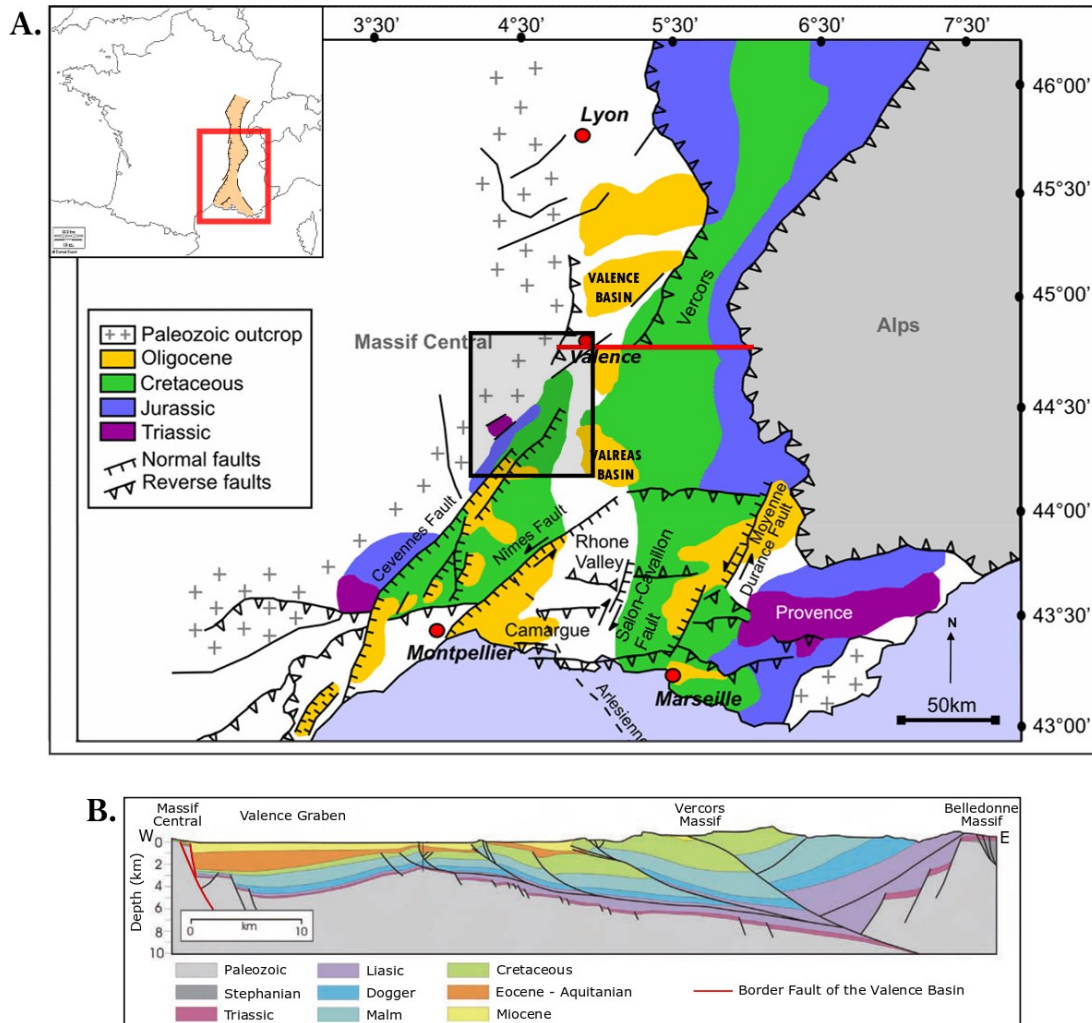


Figure 1: A. Location and simplified geological map of the South-East Basin of France (Garibaldi *et al.*, 2010). The red line indicates the location of the cross-section of the Figure 1B. The black square indicates the location of our study sites (Triassic outcrops). B. Simplified cross-section through the Valence Basin (Deville *et al.*, 1994).

2.2 Target of the geothermal projects and their analogs

Following the extensive phases of Jurassic and Oligocene periods, the continental crust in the Valence Basin area has thinned to reach a thickness of 22km (Sapin and Hirn, 1974; Guieu and Roussel, 1990). The rise up of the Moho led to an increase in the geothermal gradient to the crust scale with 4 to 4.5 °C/100m, highlighted by the work carried out by Garibaldi (2010). Indeed, this work shows positive thermal anomalies along the major faults and particularly at the southwestern edge of the Valence Basin with temperatures ranging from 170 to 195°C at 5000m deep (Garibaldi, 2010) (Figure 2).

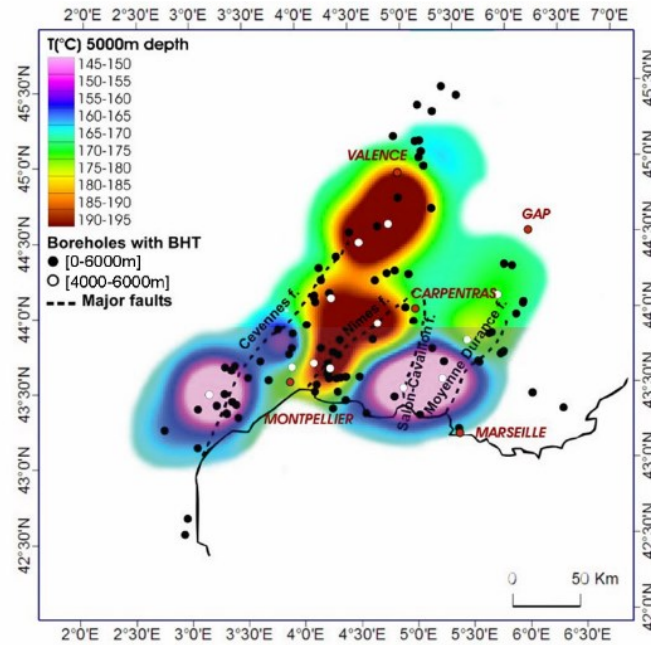


Figure 2: Thermal map of the South-East Basin of France, at 5000m depth (Garibaldi, 2010).

The sedimentary layers targeted by the deep geothermal exploitation project in the Valence Graben as potential reservoirs are the Triassic sandstones. Those sediments are located at a depth of about 4000m in the center of the graben but there are some Triassic outcrops at its western border (Figure 1A). In order to characterize the fracture network of these sandstone formations, two analog sites were chosen on the eastern border of the Massif Central for structural study: the Moulin des Vignes quarry and the Lyas quarry (Figure 3).

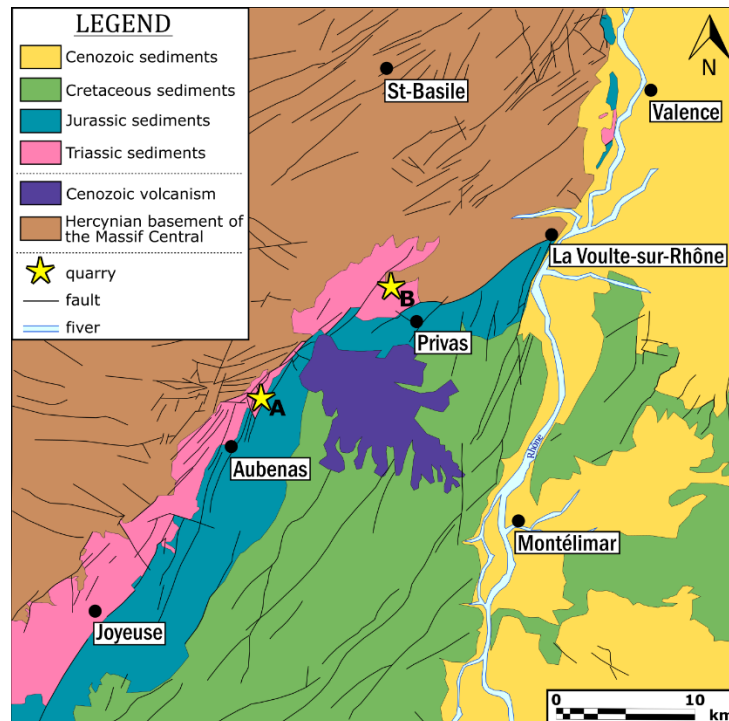


Figure 3: Simplified geological map of the western border of the Valence Basin (black square on the Figure1A). Study sites are localized. A: Moulin des Vignes quarry. B: Lyas quarry.

The Triassic formations quarried in Lyas and Moulin des Vignes are composed of medium grained arkosic sandstones deposited during middle and upper Triassic periods, respectively. Those quarries are bordered by major local faults that are indicated on the geological map of Privas at 1:50.000 scale (Ledru *et al.*, 2014):

- Moulin des Vignes quarry: faults oriented N40°E and N140°E
- Lyas quarry: faults oriented N70°E and N160°E

3. METHODOLOGY

To characterize the fracture network of the Triassic sandstone formations, we have carried out structural analysis on the two analog sites (Moulin des Vignes and Lyas quarries) by using two different methods: the classic one called the scanline method and an innovative one using a ground-based photogrammetric method.

3.1 Collection of structural measurements using the scanline method

Structural data has been collected on our analog sites by the use of the scanline method. The principle of this method is to measure and characterize every fractures spotted along a predefined line on the ground (Priest, 1993). Every structure is characterized by its orientation (dip and dip direction), position, movement, filling and other useful observations. This method helps to ensure the objectivity in the measurement and the description of structural elements on the ground (Bonnet *et al.*, 2001).

3.2 Implementation of a ground-based photogrammetric method

3.2.1 Acquisition on the ground

The ground-based photogrammetric method aims at identify the three-dimensional form of an object, like shape, dimension and position, in order to produce a virtual 3D model from photographs recording different viewpoints of this object. This method was performed within the quarries in order to produce a virtual outcrop model that most closely reflects reality.

Before conducting a photographic campaign, the targeted rock wall was prepared by the installing equipment useful for its scaling and positioning. For that, two rows of photogrammetric targets are installed to define horizontality in three dimensions (Figure 4A-B). The distance between the second row to the rock wall should always be between 20 and 100% of the width of the outcrop. Rods are also placed along the rock wall to ensure a consistent scale. Lastly, three tripods are positioned in order to obtain three different viewpoint of the whole device (Figure 4B). This redundancy is necessary for the subsequent calculations of the targets positions by triangulation. For that, the targets-tripods and tripod-tripod distances are measured using a Leica Disto laser distance meter. The targets coordinates are calculated by triangulation and are used for the georeferencing of the virtual outcrop model.

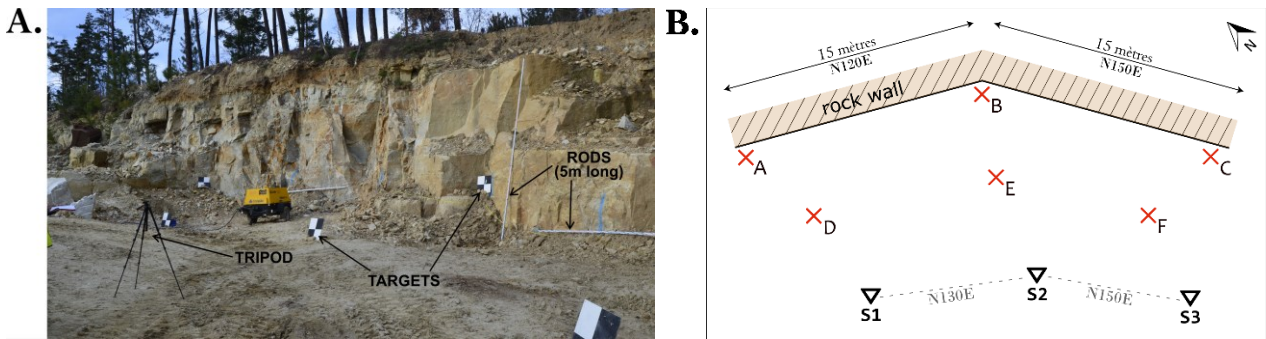


Figure 4: A. Image showing the equipment used at the Lyas quarry for the terrestrial photogrammetry campaign. B. Schematic plan of the equipment positioning (example of the Lyas quarry). Red crosses indicates the position of the photogrammetric targets. Black triangles indicates the position of the tripods.

Subsequently, the photo acquisition is performed using the “one panorama each step” method proposed by Wenzel *et al.*, (2013). ‘One panorama each step’ is a capturing approach which ensure complete coverage and sufficiently redundant observations for a very precise and reliable reconstruction of the outcrop. The principle of their approach is to acquire a panorama of the whole desired object at different viewpoints (camera stations). Camera stations used are determined according to the distance between them (the step size B) and their distance to the object (Z) (Wenzel *et al.*, 2013). These parameters can be determined as:

$$B = \frac{1}{3} H \quad (1)$$

where B , H are step size and height of the outcrop, respectively.

$$Z = \sqrt{3fB \frac{\sigma_z}{p}} \quad (2)$$

where Z is the distance station-object, f the focal length of the camera, B the step size, σ_z the precision object space, and p the pixel pitch (width).

At each station, a panorama is acquired using multiple images that are slightly overlapped.

3.2.2 Construction of the virtual outcrop model

3D digital outcrop models were built via Agisoft Metashape Professional (1.5.2) software, using images captured on the ground. Before aligning the selected images, the blurred ones have been removed. For that, the software uses an algorithm based on the principle of Structure-from-Motion (SfM) method which consists in finding the correspondences between the 2D images in order to produce a sparse 3D point cloud of the rock wall (Snavely *et al.*, 2008). Following this, the dense point cloud is calculated according

to the selected “quality” (Figure 5). The virtual outcrop model obtained is then positioned and dimensioned using the targets coordinates.



Figure 5: Virtual outcrop model of the targeted rock wall at the Lyas quarry, produced under Agisoft Metashape Professional software. The white zones corresponds to area with not enough images to reconstruct the model. The rods are 5 m long.

3.3 Structural analysis

3.3.1 Digital structural measurements

Fracture orientation measurements were performed on 3D virtual outcrop model, using the CloudCompare software (2.11 alpha) and its Compass plugin (Thiele *et al.*, 2017) which is a structural geology toolbox for the analysis of virtual outcrop models. Two main tools are available for orientation measurements:

- Plane tool: measures the orientations of fully exposed planar structures selected by hand. For that, a plane is fitting to all points sitting in the selected area and the orientation is estimate by the dip and dip direction of the plane.
- Trace tool: digitizes and measures traces and contacts produced by the intersection of the fracture plan with the rocky surface. For that, a least-cost path algorithm is used to follow the intersection trace and the digitize it to calculate its best fit plane. The orientation is given by the dip and dip direction of the calculated plane.

3.3.2 Spatial distribution

The geometric parameters of the fracture network on which we focused are the fracture orientation and the spatial distribution of fractures. The latter entails determining the inter-fractures spacing along the studied profile, using a computer program, which calculate the inter-fractures spacing of a family of orientation selected.

The results are presented graphically, using stick plots and cumulative frequency diagrams. In order to analyze the spacing distribution along a profile, we determine the coefficient of variation C_V which a dimensionless measure of the spacing variation (Gillespie *et al.*, 1993, 2001) that provides an indication of the distribution of the fractures. The value of the C_V is given by:

$$C_V = \frac{\sigma_S}{S} \quad (3)$$

where C_V , σ_S , S are coefficient of variation, standard deviation of the spacing between fractures, mean spacing, respectively.

For example, $C_V < 1$ indicates regularly spaced fractures whereas $C_V > 1$ is a characteristic of fractures that are more irregularly spaced (Sanderson *et al.*, 2019) and a profile that often displays a clustering of the fractures (Gillespie *et al.*, 1993).

4. RESULTS

4.1 Moulin des Vignes quarry

Terrestrial photogrammetric survey was conducted along a 27 m long profile oriented N30°E, by capturing 106 images of the rock wall. A total of 26 million points make up the dense point cloud on which we performed a digital scanline. 56 fracture measurements were performed on the virtual outcrop model. The global orientation of the fractures measured shows a main set oriented N140°E-N150°E (Figure 6A).

This fracture set was also analyzed in terms of spatial distribution. The average spacing is 0.532 m. Stick plot diagram allows initial visual examination of the fracture distribution on the line and the fractures seem to be regularly spaced in this case (Figure 6B). Furthermore, the cumulative frequency plot shows only minor fluctuations from the uniform distribution (Figure 6C). The C_V for the spacing is 0.82, which is < 1 . These features all indicate that the fractures are regularly spaced over 37 m with a spacing $S > 0.50$ m at a distance of ≥ 30 m distance from the fault.

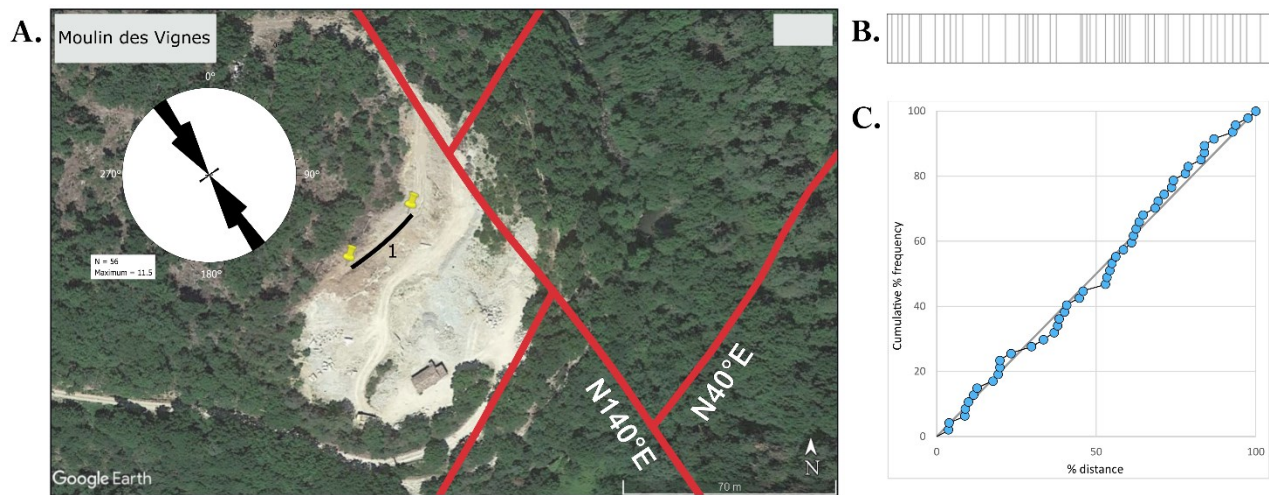


Figure 6: A. Location of the studied profile within the Moulin des Vignes quarry and direction of the fractures measured. Rose diagram of strike direction with 10° classes. Red lines represents the major faults that are indicated on the geological map of Privas at 1:50,000 scale (Ledru *et al.*, 2014). B. Spatial distribution of fractures on the line represented as stick plots. C. Cumulative plot of % frequency against % distance for the Moulin des Vignes profile. Blue circles show cumulative % frequency and diagonal line represents a uniform distribution.

By comparing the fracture orientation obtained from the scanline method (Figure 7A) and the ones obtained by the photogrammetric method (Figure 7B), we notice that there is a clear similarity. Indeed, the main fracture set is characterized by the same global direction: NW-SE.

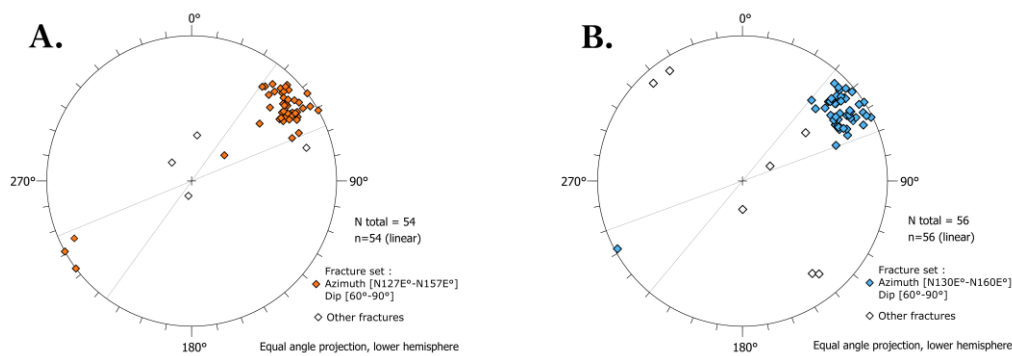


Figure 7: Results of the fracture planes measurements at the Moulin des Vignes quarry A. Stereogram showing the poles of fracture planes measured on the field by the scanline method. B. Stereogram showing the poles of fracture planes measured on the virtual outcrop model produced from the photogrammetric method.

4.2 Lyas quarry

The first profile oriented N075°E is 20 m long and starts in a crushed zone to the west. The photogrammetric campaign captured 90 images of the outcrop and a dense point cloud of 7.7 million points was built. Out of a total of 38 fracture orientations measured along this profile, we can distinguish a main fracture set oriented N170°E-N20°E (Figure 8A). The fractures positions of this fracture set along the line are represented in figure 8B on which we can observe high heterogeneity of the distribution of fractures with higher frequency at the beginning of the profile (Figure 8B). The cumulative frequency plot shows a significant irregular distribution (Figure 8C). Moreover, the C_V for the spacing is 1.33, greater than 1, indicating heterogeneity or clustering of the fractures. Indeed, we can observe a fracture corridor in the first 5 m of the line with an average spacing of 0.252 m. The 15 m that follows consists in fractures more spaced by a mean spacing $S = 1.193$ m.

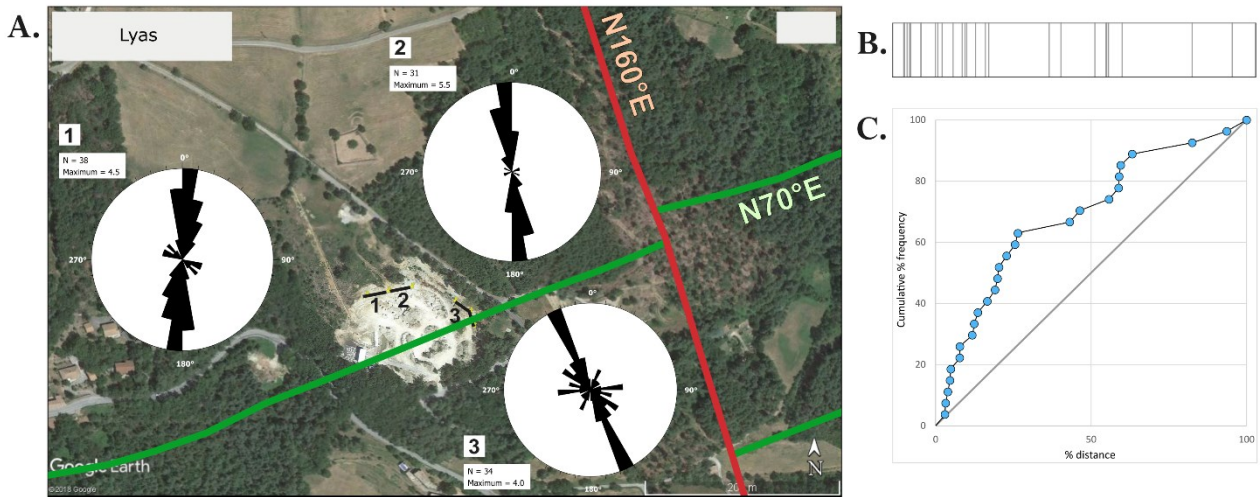


Figure 8: A. Location of the studied profile within the Lyas quarry and direction of the fractures measured. Rose diagram of strike direction with 10° classes. Green and red lines represents the major faults that are indicated on the geological map of Privas at 1:50.000 scale (Ledru *et al.*, 2014). B. Spatial distribution of fractures on the line is represented as stick plots. C. Cumulative plot of % frequency against % distance for the Lyas profile. Blue circles show cumulative % frequency and diagonal line represents a uniform distribution.

As profile n°1, the second profile is oriented $N75^\circ E$ and 20 m long. This line is the continuity of the first one. Scanline method has been applied here, for which 31 measurements were collected. A main fracture set is observed and it is globally oriented $N170^\circ E$ (Figure 8A).

A photogrammetric campaign was conducted on the third profile, which is split in two 15 m long sections: one oriented $N120^\circ E$ and another one oriented $N150^\circ E$. A dense point cloud of 5.5 million points was built from 50 images captured on the field. The digital scanline performed on the virtual outcrop model enable the collection of 34 measurements. Two fracture sets can be distinguished: the main one oriented $N150^\circ E$ - $N160^\circ E$ and a minor one oriented $N80^\circ E$ - $N90^\circ E$ (Figure 8A).

These last two profiles could not be analyzed in terms of spatial distribution of fractures due to a lack of data that would lead to a statistical bias.

Note that the orientation of the fractures rotates slightly from N-S – $N10^\circ E$ to the west to $N160^\circ E$ - $N170^\circ E$ to the east.

5. DISCUSSION

5.1 Fault interpretation

Regarding the western zone of the Lyas quarry, the field observations show a crushed corridor located west of the first profile. Furthermore, the structural data shows an increasing in fracture frequency with closeness to this zone. These features suggest us that a fault is running through this area. We propose to define the orientation of this fault according to the main fracture orientation found around this corridor, i.e. oriented N-S to $N10^\circ E$ (Figure 9).

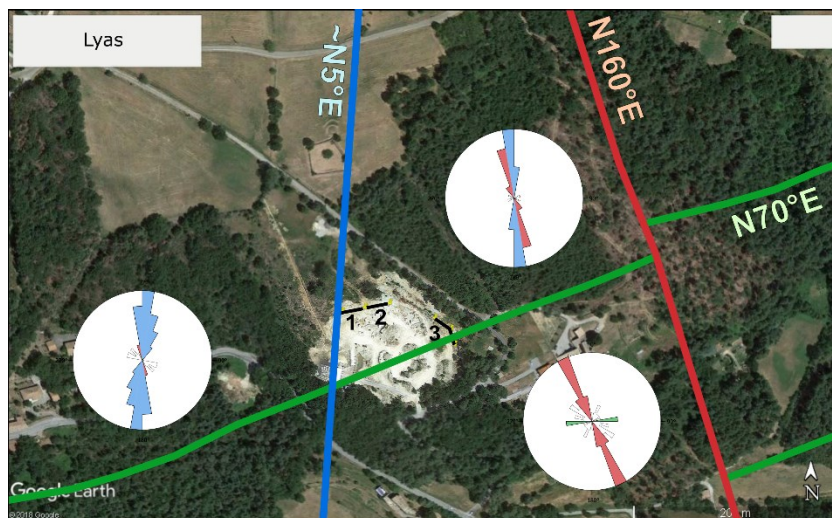


Figure 9: Location and orientation of the fault (blue line) determined from the field observations and the geometric features of the fracture network analyzed in the area. The colors of the different orientations in rose diagrams illustrates the corresponding fault.

5.2 Fracture orientation

The main fracture set highlighted in the Moulin des Vignes quarry that is oriented N140°E-N150°E coincide with the direction of the large cartographic structure oriented N140°E, bordering the north-eastern part of the quarry (Figure 6A). That strongly suggests that the fractures observed at the outcrop scale are linked to regional-scale structures. This global direction NW-SE can be associated with the N160°E normal faults created during the Tethysian rifting (Blès *et al.*, 1989; Martin and Bergerat, 1996), which are probably reactivated during the partial basin inversion (Roure *et al.*, 1992, 1994).

Regarding the results achieved in the Lyas quarry, the fracture orientations observed at the outcrop scale on the first profile are associated with the N-S to N10°E fault as noted above (Figure 9). In the eastern part of the quarry, the fractures are mostly oriented N160°E-N170°E, which correspond to the direction of the major fault oriented N160°E, located at the west side of the Lyas quarry (Figure 8A). The formation of this NNW-SSE fault is also probably due to the synsedimentary deformations during the Tethysian rifting event. The orientation of the minor fracture set observed on the third profile does not appear on the others owing to the observation bias caused by the direction of the first two profiles. The fractures of this N80°E-N90°E set, can be interpreted to Riedel shears associated with the N70°E cartographic fault located in the south of the quarry (Figure 8A). According to the Riedel shear model proposed by Cloos (1928) and Riedel (1929), the ‘R-shears’ are always present in a Riedel shear system: they are synthetic shears oriented $\sim +15^\circ$ (i.e. 15° clockwise) from the trace of right-handed strike-slip shear zones (Barlett, 1981; Davis *et al.*, 2000). This means that the N70°E cartographic structure moved in a dextral displacement. However, this fracture set is composed of a very few measurements. Our understandings from this data should therefore be interpreted with caution.

The outcome of these results is that the main fracture sets observed at the outcrop scale are linked to the orientation of the regional-scale structures present in the area. In the case of the Triassic sandstone formations on the western border of the Valence Basin, fractures are mostly oriented NW-SE to NNW-SSE according to the main faults orientation (Figure 10).

5.3 Spatial distribution of fractures

Concerning the spatial arrangement of the fractures, the results obtained on the first profile of the Lyas quarry shows that the fractures frequency is increasing with closeness to the fault. Indeed, we can consider that there is a fracture corridor at the edge of the major faults, which measures approximately 5 meters wide. Within this corridor, the mean spacing between the fractures is around 25 cm (Figure 10).

The regularity observed in the spatial organization of fractures in the Moulin des Vignes quarry, suggests that the distribution of the NNW-SSE fractures is homogeneous across several tens of meters near the major faults, after the corridor previously mentioned (Figure 10). In this regularly fractured zone, the mean spacing is > 50 cm.

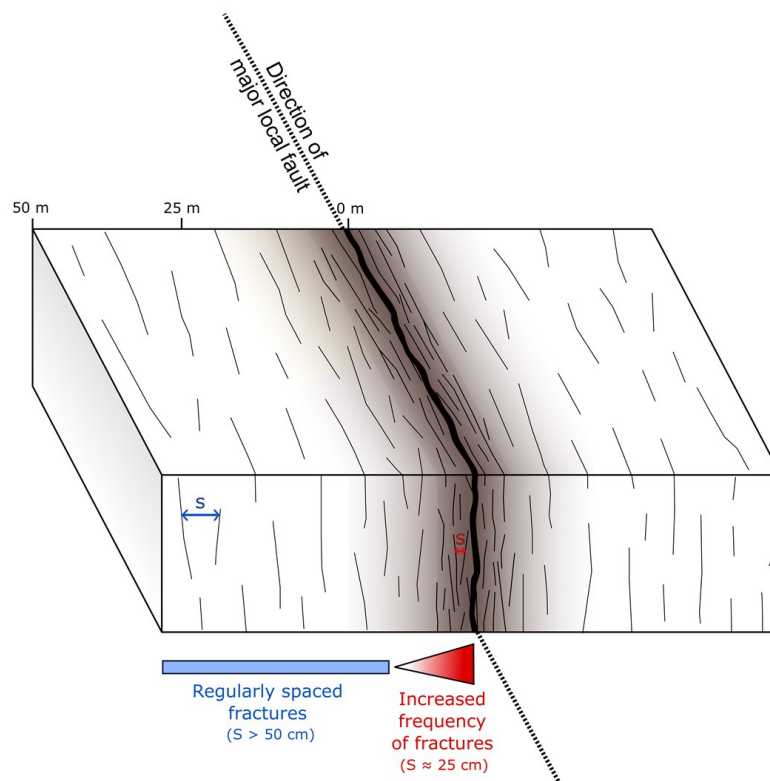


Figure 10: 3D block diagram summarizing the geometric parameters of the fracture network determined in the Triassic sandstones of the Valence Basin resulting from the photogrammetric survey.

5.4 Relevance of the photogrammetric method

This study allowed us to compare results from the field measurements (scanline method) and the digital measurements using photogrammetric method. As shown in the case of the Moulin des Vignes quarry, the results are similar with both methods (Figure 7A-B), which demonstrate the efficiency of the photogrammetric method in reconstructing an outcrop and in finding the observations found on the field.

However, digital measurements are sometimes improperly selected and miscalculated because of the observation bias and the misinterpretation of the structures. For example, it is difficult to distinguish the tectonic fractures and the decompression fractures only based on the digital model. Furthermore, the fractures only observed by their “trace” on the rock surface are an additional difficulty for the digital measurement.

Within the framework of a structural study, the main asset of the photogrammetric method is to ensure access to all parts of the targeted outcrop as long as it is covered by the photographic acquisition (like in high places). Another advantage of this method is the possibility to have an unlimited access to the virtual outcrop model in time.

6. CONCLUSION

This work reveals that the orientation of the outcrop scale fractures studied on the western edge of the Valence Basin are linked to the regional-scale structures indicated on the geological map at 1:50.000 scale. These major faults are related to the geodynamic events that occurred in the basin, such as the E-W extension of the Tethysian rifting. Thus, the main orientation pointed out in the fracture network of the Triassic sandstones is NW-SE to NNW-SSE.

Within these sandstones, we can describe the spatial distribution of the fractures bordering the major faults in two distinct parts:

- A corridor about 5 meters wide to the foot of the fault, with a mean spacing $S = 25$ cm.
- A homogeneous zone present on several tens of meters after the corridor area, with a mean spacing $S > 50$ cm.

The geometric information of the fracture network determined in this study will be used as input parameters for hydro-thermal-mechanical modelling of the geothermal reservoir. These models will allow the prediction of the fluid circulation and the heat transfer within the fractured reservoir.

The terrestrial photogrammetric method appears to be an efficient and relevant tool for the fracture measurements by the production of a virtual outcrop model. Therefore, it is an appropriate method for a structural study at the outcrop scale. Note that this digital tool is only a complementary method to the field observations.

REFERENCES

- Arthaud, F., and Matte, Ph. : Les Decrochements Tardi-Hercyniens Du Sud-Ouest de l'europe. Geometrie et Essai de Reconstitution Des Conditions de La Deformation, *Tectonophysics*, 25.1–2 (1975), 139-141,145-171.
- Bartlett, W.L., Friedman, M., and Logan, J.M. : Experimental Folding and Faulting of Rocks under Confining Pressure Part IX. Wrench Faults in Limestone Layers, *Tectonophysics*, 79.3–4 (1981), 255–77.
- Bergerat, F. : Le Couloir Rhodanien Au Paléogène; Analyse de La Fracturation et Interprétation Cinématique Régionale, *Revue de Géologie Dynamique et de Géographie Physique*, 23. fasc.5 (1982), 329–43.
- Bergerat, F., and Martin, P. : Mise En Évidence d'une Tectonique Distensive Syn-sédimentaire et Caractérisation Du Champ de Contraintes Au Trias Inférieur-Moyen Sur La Bordure Vivaro-Cévenole Du Bassin Du Sud-Est de La France; La Région de Largentière et Le Forage de Balazuc-1 (Programme Géologie Profonde de France), *Comptes Rendus de l'Académie Des Sciences*, 316 (1993), 1279–86.
- Bles, J.L., Bonijoly, D., and Gros, Y. : Successive Post-Variscan Stress Fields in the French Massif Central and Its Borders (Western European Plate): Comparison with Geodynamic Data, *Tectonophysics*, 169 (1989), 79–111.
- Bonijoly, D., Perrin, J., Roure, F., Bergerat, F., Courel, L., Elmi, S., and Mignot, A. : The Ardeche Palaeomargin of the South-East Basin of France : Mesozoic Evolution of a Part of the Tethyan Continental Margin (Geologie Profonde de La France Programme), *Marine and Petroleum Geology*, 13.6 (1996), 607–23.
- Bonnet, E., Bour, O., Odling, N.E., Davy, P., Main, I., Cowie, P., Berkowitz, B. : Scaling of Fracture Systems in Geological Media, *Reviews of Geophysics*, 39.3 (2001), 347–83.
- Choukroune, P., Le Pichon, X., and Seguret, M. : Bay of Biscay and Pyrenees, *Earth and Planetary Science Letters*, 18 (1973), 109–18.
- Cloos, H. : Experimenten Zur Inneren Tektonik, *Centralblatt Fur Mineralogie and Paleontologie 1928B*, (1928), 609.
- Davis, G.H., Bump, A.P., Garcôa, P.E., and Ahlgren, S.G. : Conjugate Riedel Deformation Band Shear Zones, *Journal of Structural Geology*, 22 (2000), 169–90.
- Deville, E., Mascle, A., Lamiroux, C., and Le Bras, A. : Tectonic Styles, Reevaluation of Plays in Southeastern France, *Oil & Gas Journal*, 92.44 (1994), 53–58.

- Garibaldi, C. : Bassin Du Sud-Est de La France et Relations Entre Anomalies Thermiques, Géologie et Circulations Hydrothermales Par Modélisation 3D (Thèse de l'Université de Nice-Sophia Antipolis, 2010).
- Gillespie, P.A., Howard, C.B., Walsh, J.J., and Watterson, J. : Measurement and Characterisation of Spatial Distributions of Fractures, *Tectonophysics*, 226 (1993), 113–41.
- Gillespie, P.A., Walsh, J.J., Watterson, J., Bonson, C.G., and Manzocchi, T. : Scaling Relationships of Joint and Vein Arrays from The Burren , Co . Clare , Ireland, *Journal of Structural Geology*, 23 (2001), 183–201.
- Guieu, G., and Roussel, J. : Conséquence Possible de l'extension Crustale Pré-Oligocène En Provence Méridionale : La Mise En Place Gravitaire Des Chevauchements, *Comptes Rendus de l'Académie Des Sciences*, Séries IIA (1990), 485–92.
- Ledru, P., Thierry, J., Marignac, C., Reboulet, S., Dagain, J., Naud, G., Roger, J., Laumonier, B., and Vernhet, Y. : Carte Géologique de France à 1/50 000, Feuille de Privas, N°841 et Sa Notice Explicative. *Édition BRGM* 188, (2014).
- Lemoine, M., Arnaud-Vanneau, A., and Arnaud, H. : Etapes et Modalités de La Subsidence d'une Paléo-Marge Passive: Les Alpes Occidentales Au Mésozoïque, *Soc. Nat. Elf Aquitaine (Production)*, (1986), 143–49.
- Lienhardt, M.J., and Pachoud, A. : Synthèse Géologique Du Bassin de Valence (26), *Rapport BRGM. Lyon : Service Géologique Régional Jura-Alpes*, (1974).
- Martin, P., and Bergerat, F. : Palaeo-Stresses Inferred from Macro- and Microfractures in the Balazuc-1 Borehole (GPF Programme). Contribution to the Tectonic Evolution of the Cevennes Border of the SE Basin of France, *Marine and Petroleum Geology*, 13.6 (1996), 671–84.
- Priest, S. : *Discontinuity Analysis for Rock Engineering* (Chapman et Hall, 1993).
- Riedel, W. : Zur Mechanik Geologischer Brucherscheinungen, *Centralblatt Fur Mineralogie and Paleontologie 1928B*, (1929), 354.
- Roure, F., Brun, J.P., Colletta, B., and Van Den Driessche, J. : Geometry and Kinematics of Extensional Structures in the Alpine Foreland Basin of Southeastern France, 14.5 (1992), 503–19.
- Roure, F., Brun, J.P., Colletta, B., and Vially, R. : Multiphase Extensional Structures, Fault Reactivation, and Petroleum Plays in the Alpine Foreland Basin of Southeastern France, *AAPG, Special Publication*, 4 (1994), 245–68.
- Sanderson, D.J., and Peacock, D.C.P. : Line Sampling of Fracture Swarms and Corridors, *Journal of Structural Geology*, 122. (2019), 27–37. DOI:10.1016/j.jsg.2019.02.006.
- Sapin, M., and Hirn, A. : Results of Explosion Seismology in the Southern Rhône Valley, *Ann. Geophys.*, 30 (1974), 181–202.
- Snavely, N., Seitz, S.M., and Szeliski, R. : Skeletal Graphs for Efficient Structure from Motion, (2008).
- Thiele, S.T., Grose, L., Samsu, A., Micklethwaite, S., Vollgger, S.A., and Cruden, A.R. : Rapid, Semi-Automatic Fracture and Contact Mapping for Point Clouds, Images and Geophysical Data, (2017), 1241–53.
- Wenzel, K., Rothmel, M., Fritsch, D., and Haala, N. : Image Acquisition and Model Selection for Multi-View Stereo, *ISPRS - International Archives of the Photogrammetry, Remote Sensing and Spatial Information Sciences*, XL-5/W1, (2013), 251–58. DOI:10.5194/isprsarchives-xl-5-w1-251-2013.
- Ziegler, P.A. : European Cenozoic Rift System, *Tectonophysics*, 208 (1992), 91–111.